JOURNAL OF MATERIALS SCIENCE 29 (1994) 6207–6211

Slip systems and plastic anisotropy in CaF_2

A. MUÑOZ, A. DOMÍNGUEZ—RODRÍGUEZ
Department Física Materia Condensada and ICMSE, Apartado 1065. 41080, Seville, Spain.
J. CASTAING
LPM-CNRS Bellevue, 92195 Meudon Cedex and Université Evry Val d' Essonne, France

An examination was made of the slip planes activated in high-purity CaF_2 single crystals with various orientations deformed by compression between 20 °C and 600 °C. It was found that {1 1 0} was the most difficult and {1 0 0} the easiest to activate. These results are compared to results for UO_2 and zirconia.

1. Introduction

A number of slip systems has been found for the deformation of CaF_2-structure crystals; the choice is dominated by electrostatic and point-defect issues [1]. All materials have the same ⟨1 1 0⟩ slip direction. In non-stoichiometric UO_2, the primary slip plane is {1 0 0} at low O/U ratios and high temperature ($T > 1673$ K), while {1 1 1} is the prevalent plane at low temperatures for all compositions and all the orientations chosen [2, 3].

A detailed study of the various slip systems has been performed for zirconia, especially on ZrO_2 which has been fully stabilized with 9.4 mol % Y_2O_3 when deformed at 1400 °C [4]. Secondary slip was activated along the {1 10} and the {1 1 1} planes; their critical resolved shear stress (CRSS) was similar and it was about 30 % higher than for the primary {1 0 0} slip plane [4].

The behaviour of CaF_2 is not modified by the large amount of point defects; this is also true for UO_2 and zirconia. The literature on CaF_2 has concluded that the primary slip planes {1 0 0} [5–9], and a secondary slip plane, {1 1 0}, plane is mentioned by several authors [6, 8, 9, 10]. In order to rationalize the knowledge on slip systems in CaF_2 compression tests were performed for a number of orientations at temperatures between 20 and 600 °C (the melting temperature $T_M = 1418$ °C = 1691 K). After determining the various slip systems which were activated, a CRSS could be ascribed at various temperatures.

2. Experimental procedures

2.1. Specimen preparation

Single crystalline CaF_2, made for infrared optics applications, was provided by SOREM (Pau, France). Compression specimens were cut using a diamond saw, after orientation by a Laue X-ray diffraction (XRD) technique. The accuracy of the orientation was better than 5°. The specimens were polished, after being cut, using diamond pastes of decreasing sizes down to 3 μm. The mechanical tests were then performed with no other step in the process, except for the thermal equilibration of the furnace (1–2 h at the test temperature).

The specimen sizes were close to $3 \times 3 \times 6$ mm^3, and they had the orientations depicted in Table I. They were chosen to be analogous to specimens in previous works on UO_2 [2, 3] and zirconia [4], in order to achieve different Schmid factors f (Table I).

2.2. Mechanical tests

Compression tests were conducted at a constant strain rate $\dot{\varepsilon} \simeq 1.4 \times 10^{-5}$ s^{-1} in an Instron machine equipped with an electrical furnace operating in air. Tests were performed at temperatures between 20 and 600 °C.

Engineering stress σ, versus strain, ε, curves were deduced from force–time curves. The shear stress, τ and the shear strain γ were calculated as $\tau = \sigma f$ and $\gamma = \varepsilon/f$; these values are valid at small deformations.

In the data plotted in the Figures 5–7, we have not deduced the elasticity of the testing equipment, which is of the order of 17.9 N μm^{-1} (the force–displacement ratio).

The CRSS were taken on σ–ε curves at the offset from linear behaviour.

2.3. Observations of specimens

Optical reflection microscopy was used to detect slip

TABLE I Crystallographic data for the various orientations of CaF_2 single crystals and the corresponding Schmid factors f, for the different slip planes and the variqus ⟨1 $\bar{1}$ 0⟩ slip directions

Compression axis	Lateral faces		Schmid factors for slip planes		
			{100}	{110}	{111}
⟨001⟩	(1 $\bar{1}$ 0)	(1 1 0)	0.00	0.50	0.41
⟨115⟩	(5 5 $\bar{2}$)	(1 $\bar{1}$ 0)	0.26	0.44	0.45
⟨113⟩	(3 3 $\bar{2}$)	(1 $\bar{1}$ 0)	0.39	0.36	0.45
⟨112⟩	(1 1 $\bar{1}$)	(1 $\bar{1}$ 0)	0.47	0.25	0.41
⟨011⟩	(1 1 $\bar{1}$)	(2 $\bar{1}$ 1)	0.35	0.25	0.41

0022–2461

lines on the lateral faces of the specimens. Contrasts were difficult to obtain because of the transparency of the CaF_2 crystals. This could be achieved by using low-intensity illumination and defocusing the microscope from the surface. In such conditions, it was possible to reveal slip bands even when the dislocations did not leave steps because their Burgers vectors were parallel to the surface.

The angles between the slip bands and a reference axis were measured and used to determine the slip planes by using stereographic projections.

3. Results

3.1. Determination of the slip systems

Our experiments allowed the slip planes to be determined, with some indication of the slip direction; no steps were expected when the slip direction was parallel to the observed surface. There were no indication of directions other than the usual $\langle 1\,1\,0 \rangle$ directions.

The common $\{1\,0\,0\}$ plane has been observed for many experimental conditions (Table II). An example is shown in Fig. 1 where the $\{1\,0\,0\}$ plane was activated at room temperature. Slip lines are well contrasted in the $(5\,5\,\bar{2})$ face of this specimen deformed along $\langle 1\,1\,5 \rangle$; we concluded that this was because of the activation of the $(0\,0\,1)$ $[1\,1\,0]$ slip at room temperature.

For specimens compressed along $\langle 1\,1\,3 \rangle$, the slip lines in the $(3\,3\,\bar{2})$ faces are very similar to the slip lines displayed in Fig. 1, corresponding to the $(0\,0\,1)$ $[1\,1\,0]$ slip. Strong contrasts are visible on the orthogonal faces (Fig. 2), but they do not correspond to any step at the surface. This indicates that the slip direction is parallel to $[1\,1\,0]$. The lines in Fig. 2 correspond, around the edge of the specimen, to lines which are perpendicular to the compression axis in the $(3\,3\,\bar{2})$ face. This allows the conclusion to be made that only one slip plane has been activated.

For specimens deformed along $\langle 0\,0\,1 \rangle$, slip planes of the $\{1\,0\,0\}$ type cannot be activated (Table I). We expect either $\{1\,1\,1\}$ or $\{1\,1\,0\}$ planes. We chose the $\{1\,1\,0\}$ lateral faces, which allowed us to distinguish between the two slip planes. A specimen deformed by 0.4 % at 183 °C displayed a few contrasted lines perpendicular to the compression axis. Other faint lines were detected either perpendicular or at 32–39° to $\langle 0\,0\,1 \rangle$ (Fig. 3), so it can be concluded that the $\{1\,1\,1\}$ planes had been activated.

TABLE II The slip planes which are observed for CaF_2 when it is deformed at various temperatures and compression directions

Compression axis	Slip planes at various temperatures, T		
	$T = 20$ °C	$90 < T < 400$ °C	$400 < T < 600$ °C
$\langle 0\,0\,1 \rangle$	F[a]	$\{1\,1\,1\}$	$\{1\,1\,0\}$
$\langle 1\,1\,5 \rangle$	$\{1\,0\,0\}$	$\{1\,0\,0\}$	$\{1\,1\,1\}$
$\langle 1\,1\,3 \rangle$	$\{1\,0\,0\}$ + F[a]	$\{1\,0\,0\}$	$\{1\,0\,0\}$
$\langle 1\,1\,2 \rangle$	F[a]	$\{1\,0\,0\}$	$\{1\,0\,0\}$
$\langle 0\,1\,1 \rangle$	$\{1\,0\,0\}$	$\{1\,0\,0\}$	$\{1\,0\,0\}$

[a]F indicates fracture.

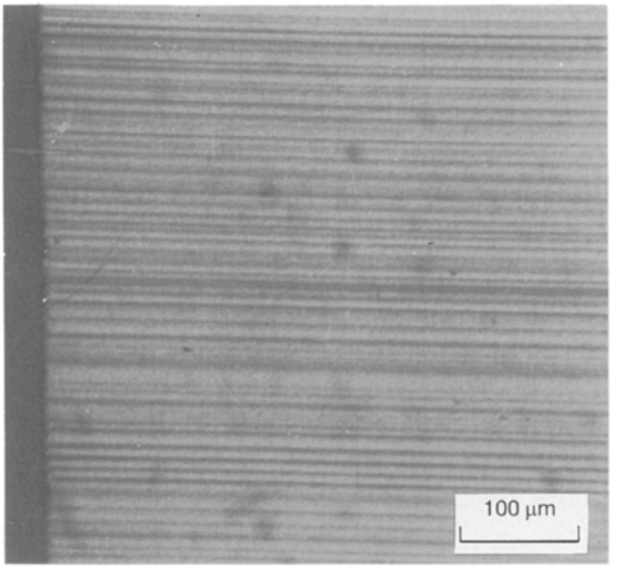

Figure 1 Slip lines on a $(5\,5\,\bar{2})$ face of a specimen deformed along $[1\,1\,5]$ at room temperature ($\varepsilon = 0.38\%$). The visible edge of the specimen is parallel to the compression axis.

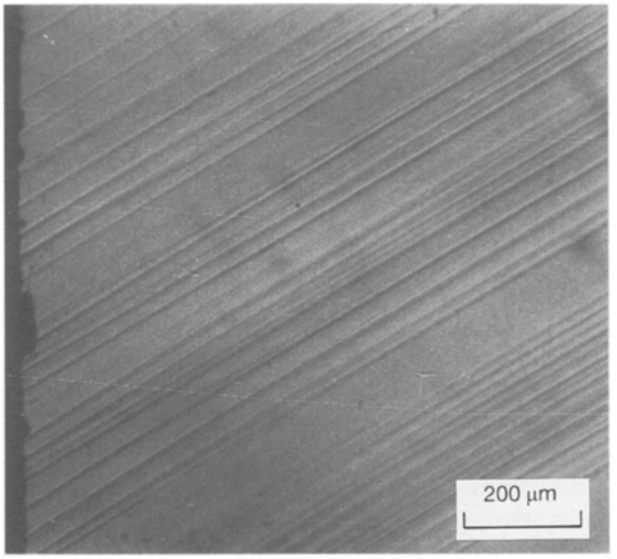

Figure 2 Slip lines on a $(1\,\bar{1}\,0)$ face of a specimen deformed along $[1\,1\,3]$ at $T = 136$ °C and $\varepsilon = 1.62\%$. The visible edge of the specimen is parallel to the compression axis. Here, the contrast is due to dislocation stresses affecting the optical properties of CaF_2.

The $\{1\,1\,1\}$ $\langle 1\,1\,0 \rangle$ slip system was also activated for the $\langle 1\,1\,5 \rangle$ compression axis for high temperatures $T \geq 462$ °C ($0.43\,T_M$).

For the same orientation at 600 °C only lines at 55–60° from the $\langle 0\,0\,1 \rangle$ compression axis were observed (Fig. 4); this was attributed to the $\{1\,1\,0\}$ slip. The lines are fairly straight for such a high-temperature deformation.

After compression at room temperature along $\langle 0\,1\,1 \rangle$, the specimens tended to cleave along a $\{1\,1\,1\}$ plane parallel to the compression axis. The faces were covered with several sets of faint lines. The $\{1\,0\,0\}$ planes were identified, as was expected from the previous observations.

The slip planes observed for the various experimental conditions are summarized in the Table II. The $\{0\,0\,1\}$ planes are the most frequent.

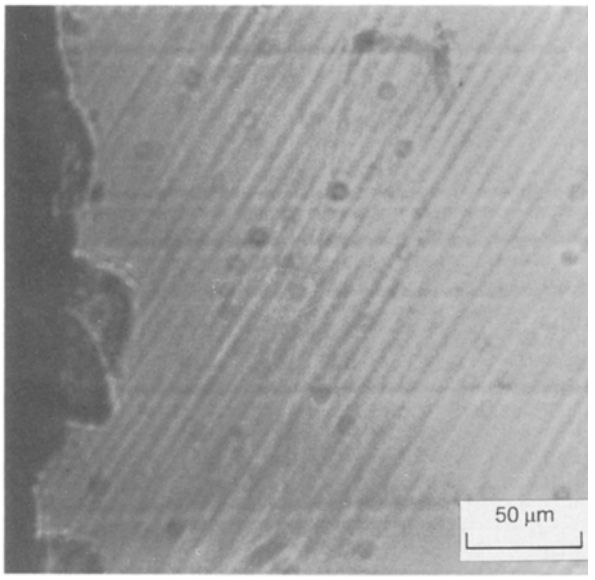

Figure 3 Slip lines for a specimen deformed at 183 °C along [0 0 1] ($\varepsilon = 0.4\%$). The edge of the specimen is parallel to the compression axis. The observation was of a (1 1 0) face. Similar lines were observed in the orthogonal lateral face.

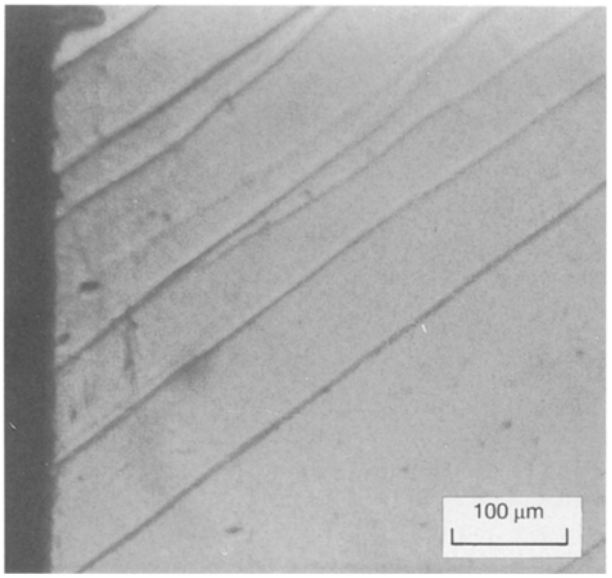

Figure 4 Slip lines for a specimen deformed at 600 °C along [0 0 1] ($\varepsilon = 0.85\%$). The edge of the specimen is parallel to the compression axis. The observation was of (1 1 0) face. Similar lines were observed in the orthogonal lateral face.

3.2. The stress-strain behaviour

A number of stress–strain curves are given in Figs 5, 6 and 7 with axes τ–γ. They display a parabolic behaviour which was not found in the results of other authors [7]. The change from elastic behaviour to plasticity is gradual; a large work-hardening rate is observed for all orientations, which is typical of multiple slip. The scatter in the gradients of the elastic stage is due to possible misalignment of the experimental set-up.

The curves are shown for various orientations of the compression axis for the {1 0 0} slip in Fig. 5. Plastic yielding happens at the same value of stress for $T = 136$ °C.

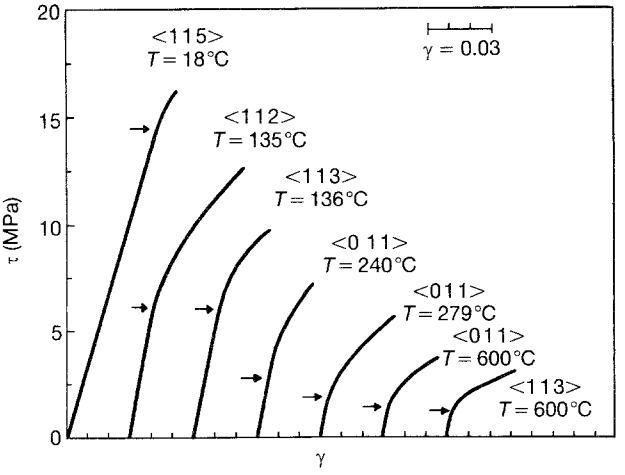

Figure 5 The resolved stress, τ and strain, γ, for the deformation of CaF_2 crystals along different compression directions at various temperatures. All the tests corresponded to the {1 0 0} slip.

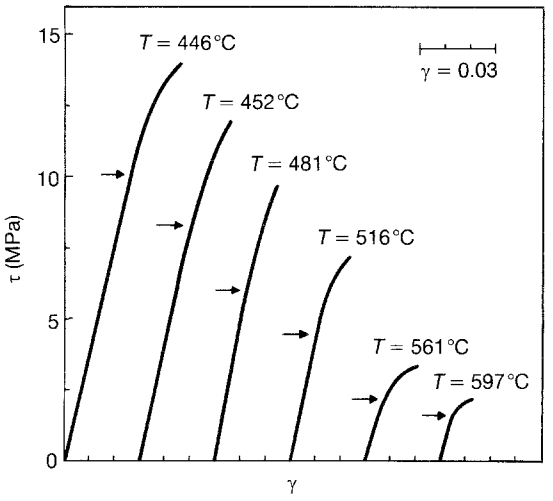

Figure 6 τ–γ curves for compression along ⟨0 0 1⟩ at various temperatures. The {1 1 0} slip was activated.

The activation of the {1 1 0} planes has been obtained for a single orientation of the compression axis (Table II) when {1 1 1} corresponded to two orientations. High temperatures were required for these planes, that is, 446 °C ($0.43T_M$, Fig. 6) and 183 °C ($0.27T_M$, Fig. 7), respectively.

In all τ–γ curves, the work-hardening rates are high, in spite of the high temperature of the deformation.

3.3. The critical resolved shear stress

The CRSS is plotted in Fig. 8. The values of the CRSS, deduced directly from Instron charts, are shown in Figs 5, 6 and 7 by arrows.

The plot in Fig. 8 gathers values obtained for different orientations of the stress for {1 0 0} and {1 1 1} slip. The good agreement of the results indicates that the Schmid law is obeyed for these slip planes.

The easiest slip plane is {1 0 0} which is athermal above 300 °C ($0.34T_M$) (Fig. 8) and it can be activated at room temperature (which was the lowest temperature for plastic deformation without failure in our tests).

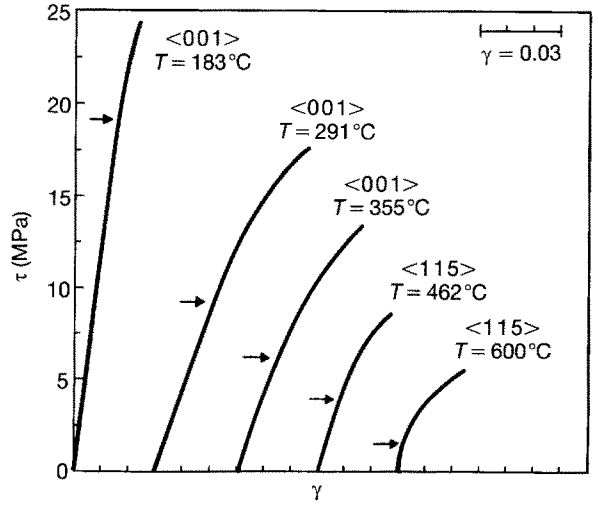

Figure 7 τ–γ curves for compression along ⟨0 0 1⟩ at $T \leq 355\,°C$ and along ⟨1 1 5⟩ at $T \geq 462\,°C$. For all the curves, the {1 1 1} slip plane was activated.

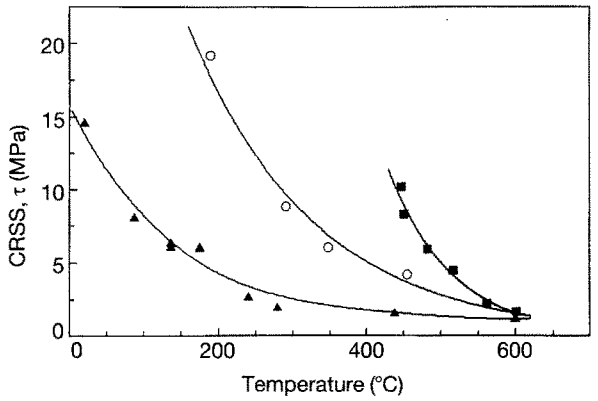

Figure 8 The CRSS-versus-temperature curve for different slip systems: (▲) {1 0 0}, (○) {1 1 1}, and (■) {1 1 0}. Values obtained from different orientations of the stress.

The {1 1 1} slip plane is the second strongest plane (Fig. 8), {1 1 0} being the hardest. The CRSSs of these systems are thermally activated up to 600 °C ($0.52T_M$), where they have the same value as {1 0 0}. Plasticity is isotropic at 600 °C and it is very likely that it is isotropic above this temperature.

4. Discussion

4.1. Mechanical data

CaF_2 was deformed down to room temperature and a CRSS of $\tau = 15$ MPa was found (Fig. 8) ($\tau/\mu = 3.5 \times 10^{-4}$, and $\mu = 4.3 \times 10^{10}$ Pa deduced from [11]).

Previous works [5–8] have not reached such a low temperature, and they all found higher values for the CRSS of the {1 0 0} planes than are presented here. This is probably because materials of lower purity were used.

The only existing mechanical data attempting a plastic anisotropy study are those of Baudinaud [8], who performed compression tests along the ⟨0 0 1⟩ and ⟨0 1 1⟩ directions between $T = 300\,°C$ and $T = 800\,°C$. He found a small anisotropy in the yield stresses, up to the highest temperatures; this contrasts with our results (Fig. 8). His yield-stress value for the softest orientation (σ//⟨0 1 1⟩) at 300 °C is surprisingly high ($\sigma/\mu = 4.34 \times 10^{-4}$ or $\sigma = 18.7$ MPa) when compared with our results (Fig. 8) and with those of Evans and Pratt [7]. Unfortunately, the specimens that Baudinaud used contained a high level of impurities [8]; this explains the discrepancy.

The thermal activation of the {1 0 0} CRSS that we found (Fig. 8) is similar to that found by Evans and Pratt [7]; they attributed this to dislocation–point-defect interactions [6]. Since our specimens were softer than theirs, we concluded that they had a lower impurity content, but that similar point defects still control the glide of charged dislocations.

For the secondary {1 1 1} and {1 1 0} systems, the thermal activation is stronger than for the {1 0 0} system (Fig. 8); this is probably because of the higher electrostatic interactions between the point defects and the dislocations.

4.2. Slip systems

We have found that {1 0 0} is the primary slip system in CaF_2, in agreement with previous authors [5–9]. The secondary {1 1 0} plane has been mentioned by a few authors [8–10]; we found that it was more difficult to activate than the {1 1 1} plane (Fig. 8), and it may have been activated but not observed in other works. Specimens with {1 0 0} lateral faces give slip lines at 45° from the ⟨0 0 1⟩ compression axis for both the {1 1 0} and the {1 1 1} planes. This is the usual condition for experiments, which have concluded to {1 1 0} slip planes, by analogy to NaCl structure crystals and probably because the Schmid factor is higher (0.5).

In order to have unambiguous determination of slip planes, we cut specimens with {1 1 0} lateral faces. In this case, the {1 1 0} and {1 1 1} planes give different slip lines in the lateral faces. We definitely identified that {1 1 1} is the secondary slip (Table II, Figs 4 and 7) and that {1 1 0} is activated in specific conditions (Table II, Fig. 6).

The sequence of increasing strength for slip on {1 0 0}, {1 1 1} and {1 1 0} planes is well established for CaF_2. This sequence is also valid for UO_2 and ZrO_2, with some adjustments depending on the amount of point defects.

At high temperatures, {1 1 1} and {1 1 0} are present as secondary planes in zirconia [1, 4] and in UO_2 [2]. When the ratio O/U increases, the CRSS for {1 1 1} decreases and it can reach the value for {1 0 0}. This behaviour corresponds to high-temperature experiments, where the plastic anisotropy is small and the Schmid-factor values are dominant.

At low temperature, UO_2 was found to slip on {1 1 1} planes [3], in contrast to CaF_2, and both the {1 0 0} and the {1 1 1} planes could be activated in zirconia [1], particularly under microindentation [12–13]

Slip in CaF_2-structure crystals occurs mostly along the {1 0 0} and {1 1 1} planes, {1 1 0} being the hardest plane.

4.3. Plastic anisotropy

Plastic anisotropy is particularly important at low temperatures when the deformation is thermally activated (Fig. 8). Various criteria may be used to explain the ranking of the CRSS for various crystallographic planes [14]. Elastic-energy considerations did not allow a rationalization of the ranking of the slip systems in ZrO_2 [1]. CaF_2 being more isotropic than ZrO_2 elasticity does not allow its slip behaviour to be explained (Table II).

The Peierls mechanism is not able to explain our results since it predicts that {1 1 0} should be the easiest slip plane [1] which does not agree with experimental observations (Fig. 8).

Electrostatic issues at the dislocation core lead Domínguez-Rodriguez *et al.* to conclude that {1 1 0} should be the most difficult and {1 0 0} the easiest [1]; this agrees with the present results. The basis of the prediction is the distances between unlike ions or identical ions for the half-slipped position. Such an approach is valid for CaF_2 which contains a small amount of impurities. In the cases of UO_2 and zirconia, the large amount of point defects alters the distribution of the ions at the dislocation cores; this prevents the application of the model mentioned above. This explains why the sequence of CRSS for the {1 0 0}, {1 1 1} and {1 1 0} planes is not so well followed for UO_2 and zirconia as it is for CaF_2.

Acknowledgement

The authors wish to thank M. Brun (SOREM, Pau, France) who provided good-quality CaF_2 crystals.

References

1. A. DOMÍNGUEZ-RODRÍGUEZ, A. H. HEUER and J. CASTAING, *Radiation Effects and Defects in Solids* **119–121** (1991) 759.
2. R. J. KELLER, T. E. MITCHELL and A. H. HEUER, *Acta Metall.* **36** (1988) 1073.
3. *Idem., ibid.* **36** (1988) 1061.
4. A. DOMÍNGUEZ-RODRÍGUEZ, D. S. CHEONG and A. H. HEUER, *Phil. Mag. A* **64** (1991) 923.
5. W. L. PHILLIPS, Jr., *J. Amer. Ceram. Soc.* **44** (1961) 499.
6. A. G. EVANS and P. L. PRATT, *Phil. Mag.* **20** (1969) 1213.
7. *Idem., ibid.* **21** (1970) 951.
8. V. BAUDINAUD, Thesis, Contribution á l'étude de la déformation plastique de la fluorine, Poitiers, France (1978).
9. W. M. SHERRY and J. B. VANDER SANDE, *Phil. Mag. A* **40** (1979) 77.
10. P. FELTHAM and R. GHOSH, *Phys. Status Solidi (a)* **5** (1971) 279.
11. R. K. SINGH, S. S. MITRA and C. N. RAO, *Phys. Rev. B* **44** (1991) 838.
12. G. N. MORSCHER, P. PIROUZ and A. H. HEUER, *J. Amer. Ceram. Soc.* **74** (1991) 491.
13. A. PAJARES, F. GUIBERTEAU, A. DOMÍNGUEZ-RODRÍGUEZ and A. H. HEUER, *J. Amer. Ceram. Soc.* **74** (1991) 859.
14. T. BRETHEAU, J. CASTAING, J. RABIER and P. VEYSSIERE, *Adv. Phys.* **28** (1979) 829.

Received 5 August 1993
and accepted 16 May 1994